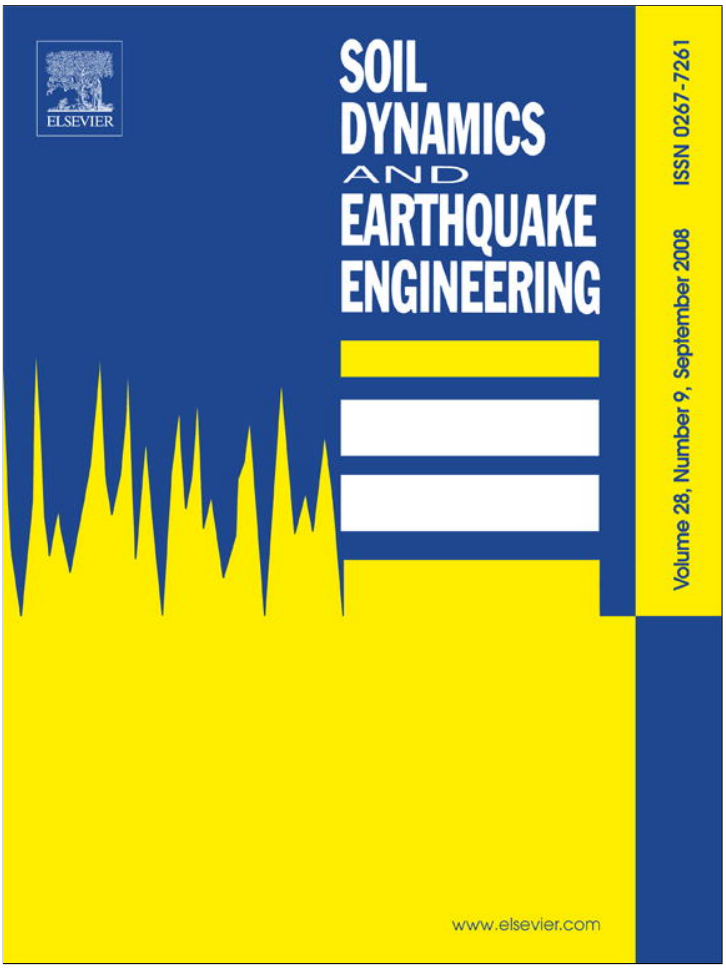

ELSEVIER

Soil Dynamics and Earthquake Engineering 28 (2008) 738–753

SOIL DYNAMICS AND EARTHQUAKE ENGINEERING

www.elsevier.com/locate/soildyn

Evaluation of near-source seismic records based on damage potential parameters Case study: Greece

Constantine C. Spyrakos*, Charilaos A. Maniatakis, John Taflambas

Department of Civil Engineering, Laboratory for Earthquake Engineering, National Technical University of Athens, GR-15700 Zografos, Athens, Greece

Received 1 October 2007; accepted 6 October 2007

Abstract

The study presents the results of an investigation that identifies among the available records in Greece those that reveal near-source characteristics, using a procedure based on damage potential parameters. The findings reaffirm the opinion that earthquakes with magnitude less than $M = 6.0$ present near-source phenomena that can cause severe damage to relatively stiff structures, common in urban areas. Spectra from selected accelerograms of near-source records are compared with the corresponding elastic spectra of the current Greek Seismic Code, (EAK 2000), the impulsive character of the Greek near-source records is ascertained and shortcomings of EAK 2000 to account for near-source effects are demonstrated.

Based on records from seismic events in Greece and records from international earthquakes of small-to-moderate magnitude, the study demonstrates that there exists a near-source magnitude-distance region, where the velocity pulses have smaller amplitude and period in comparison with earthquakes of great magnitude. A simplified representation of three pulse types is, also, adopted for near-source events. It is found that the type-A pulse related to permanent displacement phenomena does not characterize Greek records. In addition a simple criterion is developed to identify the most appropriate simplified pulse type for near-source seismic events independently of magnitude.

Keywords: Near-source region; Seismic damage criteria; Strong ground motion; Earthquake engineering; Impulsive seismic motion

1. Introduction

There has been an increasing interest to study near-source phenomena since the earthquake of 1966, in Parkfield, California [1]. Also, in the strike-normal component of Pacoima Dam record of the 1971 earthquake in San Fernando, it was ascertained that significant period velocity pulses could be present in the near-source records and an effort was made to simulate the strong motion with reductive models [2]. The importance of the near-source motion characteristics on the elastic and inelastic behaviour of engineered structures has been noted by several researchers, i.e. Bertero et al. [3], Naeim [4], Makris [5], Chopra and Chintanapakdee [6], Mavroeidis et al. [7]. The sensitivity of flexible or base isolated structures accommodating the deformation demands of the impulsive motion in the near-source region has also been addressed in several studies, e.g., Hall et al. [13]. Using simplified mathematical models Ricker [9], Gabor [10], Hudson [11] and Mavroeidis and Papageorgiou [12] have proposed a quite extended range of wavelets to examine impulsive ground-motion.

It is broadly accepted that the most severe damage from earthquake activity is localized in a region close to the causative fault, known as the "near-source". Significant damage can also occur far from the energy release when there exist unusual local site effects. The expected acceleration amplitude of the ground motion is strongly related to the focal depth of small-to-moderate magnitude earthquakes in short distances from the source [13]. The shallower the earthquake the more damaging it is expected

*Corresponding author. Tel.: +30 210 772 1187; fax: +30 210 772 1182.
E-mail address: spyrakos@hol.gr (C.C. Spyrakos).

0267-7261/$ - see front matter © 2007 Published by Elsevier Ltd.
doi:10.1016/j.soildyn.2007.10.003

to be near the source. Also, significant vertical accelerations are expected to develop, a parameter that increases the possibility of severe damage, a remark made by several researchers, e.g., Elnashai and Papazoglou [14]. Somerville et al. [15] indicated that the damage potential in the near-source region is greatly affected by phenomena related with the propagation of the fault rupture, such as polarization and directivity effects. Velocity pulses of significant amplitude have been related with the hazard induced by strong motion, specially when combined by large displacement demands. Unfortunately the processing of the strong motion data usually distorts the acceleration earthquake signal in the low-frequency region unless a special procedure is employed, such as the one applied in the Lucerne Valley record by Iwan and Chen [16], to estimate the real displacement demand. An examination of filtering procedures has led to the conclusion that the combined application of baseline and filtering can provide the optimum results [17].

Rupture directivity is found to increase the low-frequency content of ground motion at distances within 20 km from the focus [18,19]. From the performance-based design point of view, the impulsive motion induced by forward rupture directivity is found to amplify the spectral scaling factors of displacement specified by current codes for a wide range of frequencies [20]. The study of the effects of rupture directivity on ground-motion attenuation relationships has led to the conclusion that the period of the pulse increases with magnitude, a parameter related with fault dimensions and source parameters [15,21–23]. Therefore, the amplification effect of impulsive motion is limited to a narrow region near the prominent period of the pulse. Small-to-moderate earthquakes are expected to have peaks in their elastic response spectra at higher frequencies, affecting structures with a medium fundamental period as compared with earthquakes of greater magnitude with long period pulses in their near-source records. Although the directivity effect has been thought as limited to earthquake magnitudes greater than M6.0, it has been ascertained that it can play a significant role in seismic events of smaller amplitude [22,24].

Even though the importance of near-source phenomena is well known, there is no clear definition of the distance-magnitude relation which constitutes the far-fault boundary. Several definitions have been given by, e.g., Campbell [25], Bolt and Abrahamson [26], Krinitzky and Chang [27], Hudson [28], Ambraseys and Menu [29], Bommer [30], Martinez-Pereira and Bommer [31], Martinez-Pereira [32], who have made an effort to determine the distance-magnitude boundary based on near-fault records from destructive earthquakes. Several parameters, such as PGA and Arias intensity, have been used in order to study the amplitude, energy, frequency content and duration of the strong motion records [32,33].

In a previous work [34], the authors presented an evaluation of near-source records in Greece. In this study: (i) the impulsive character of near-source motion in Greece is studied, (ii) comparisons with international seismic near-source records are made and conclusions are drawn, and (iii) the possibility of recognition of the pulse type by means of simple criteria is examined. The study also demonstrates the need for further research that will lead to design procedures to account for near-source effects of small-to-moderate earthquakes.

2. Source of data

In the present study the accelerograms are obtained from the databases of the Geodynamic Institute of the National Observatory of Athens (GI-NOA) [35] and the unified database of GI-NOA and the Institute of Engineering Seismology and Earthquake Engineering (ITSAK) [36]. Records of international seismic events have been downloaded from PEER [37], COSMOS Virtual Data Center [38] and NGDC Strong Motion Databases [39]. The Greek data extend for the period from 1973 to 1999, a total of 860 ground-motion records.

The majority of available accelerograms has been recorded at soil conditions characterized by relatively poor mechanical properties. The classification of the soil conditions of the stations is different between the two Greek databases. The GI-NOA gives detailed annotations about the geology of each one of its 57 stations [35]. The unified GI-NOA and ITSAK database uses the two different kinds of soil classification as shown in Fig. 1, where the percentage of the recorded accelerograms obtained for each soil category is presented. The classification shown in Fig. 1(a) consists of four soil-types, i.e., A, B, C and D compatible with the Greek Seismic Code EAK 2000 [40]. The second classification consists of three categories, which are: type 0, 1 and 2, (Fig. 1(b)), with soil type 0 corresponding to type-A and type-B, soil type 1 corresponding to type-C and soil type 2 corresponding to type-D soil conditions.

The description of the stratigraphic profile for each soil category according to EAK 2000 [40] and the Eurocode 8 [41] as well their correlation is presented in Table 1. Details about the instruments used by ITSAK,

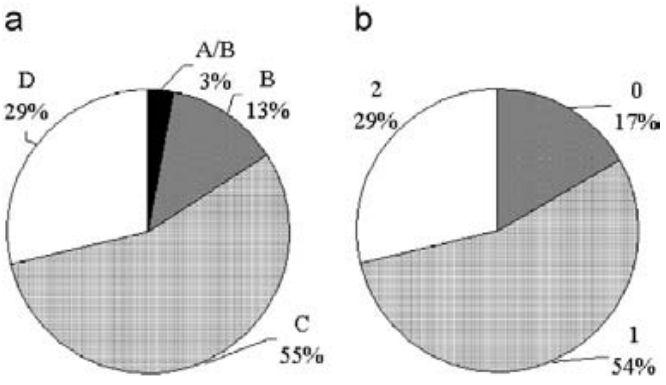

Fig. 1. Distribution of the unified GI-NOA and ITSAK database for soil classification: (a) first classification and (b) second classification.

Table 1
Correlation between EAK 2000 and EC8 for soil classification

Soil classification			
Greek Aseismic Code (EAK 2000)		Eurocode 8 (EC8)	
A	• Rock or rock-like formations extending in wide area and large depth provided that they are not strongly weathered • Layers of dense granular material with little percentage of silty-clayey mixtures, having thickness less than 70 m • Layers of stiff overconsolidated clay with thickness less than 70 m	A	Rock or other rock-like geological formation, including at most 5 m of weaker material at the surface ($v_{s,30}>800$ m/s)
B	• Strongly weathered rocks or soils which can be considered as granular materials in terms of their mechanical properties • Layers of granular material of medium density with thickness larger than 5 m or of high density with thickness over 70 m • Layers of stiff overconsolidated clay with thickness over than 70 m	B	Deposits of very dense sand, gravel, or very stiff clay, at least several tens of meters in thickness, characterized by a gradual increase of mechanical properties with depth ($360<v_{s,30}<800$ m/s).
		C	Deep deposits of dense or medium-dense sand, gravel or stiff clay with thickness from several tens to many hundreds of meters ($180<v_{s,30}<360$ m/s)
C	• Layers of granular material of low relative density with thickness over 5 m or of medium density with thickness over 70 m • Silty-clayey soils of low strength with thickness over 5 m	D	Deposits of loose-to-medium cohesionless soil (with or without some soft cohesive layers), or of predominantly soft-to-firm cohesive soil ($v_{s,30}<180$ m/s)
		E	A soft profile consisting of a surface alluvium layer with v_s values of type C or D and thickness varying between about 5 and 20 m, underlain by stiffer material with $v_{s,30}>800$ m/s
D	Soft clays of high plasticity index ($I_p>60$) with total thickness over 12 m	S_1	Deposits consisting, or containing a layer at least 10 m thick, of soft clays/silts with a high plasticity index (PI > 40) and high water content ($v_{s,30}<100$ m/s)
X	• Loose fine-grained silty-sandy soils under the water table which may liquefy (unless a specific study proves that such a hazard can be excluded or their mechanical characteristics will be improved) • Soils which are close to apparent tectonic faults • Steep slopes covered with loose debris • Loose granular soils or soft silty-clayey soils, which have been proved hazardous in terms of dynamic compaction or loss of strength • Recent loose backfills. Organic soils • Soils of class C with excessively steep inclination	S_2	Deposits of liquefiable soils, of sensitive clays, or any other soil profile not included in types A–E or S_1

$V_{s,30}$: average shear wave velocity (Eurocode 8, equation (3.1)).

GI-NOA, PEER, COSMOS and NGDC databases are provided in references [35–39].

3. Criteria for near-source records

In order to evaluate the characteristics of the near-source region a procedure primarily based on the work of Martinez-Pereira and Bommer [31] is adopted. According to this procedure criteria have been established to select the records that could cause ground motion intensity of Modified Mercalli scale (MMI) greater than or equal to VIII. The criteria are based on the lower bounds of ground motion parameters correlated with MMI greater than or equal to VIII. From the magnitude-distance relation of the records that satisfy all criteria, a near-source region is defined outside which seismic events, even if characterized by directivity phenomena, are not expected to exceed intensity values of VIII, unless local site effects dominate the response. However, inside the region the presence of lower amplitude records is not excluded. The criteria define the near-source region in which even well engineered structures could suffer significant damage. The parameters used to select the records attempt to address the complexity of strong seismic motion, such as frequency content, amplitude and duration, given the fact that it is impossible to characterize strong motion accurately using any single parameter [42].

The six parameters listed in Table 2 have been selected to characterize salient features of strong motion, that is, peak horizontal ground acceleration (PHGA) [8], cumulative absolute velocity (CAV), peak horizontal ground velocity (PHGV), Arias intensity (I_A), the damage potential

parameter proposed by Fajfar et al. [43], (I), and the root mean square acceleration (a_{rms}).

The *PHGA* is probably the most widely used parameter to characterize ground motion. The lower bound for ground-motion acceleration correlated to MMI intensities VIII is PHGA equal to $0.2g$ [31]. This lower bound is in compliance with the US National Research Council provisions [44].

Table 2
Strong-motion parameters and measured characteristics

Ground motion parameters	Ground motion characteristics				Lower bound
	Amplitude	Frequency content	Duration	Energy	
PGA	✓				$0.2g$
CAV	✓			✓	$0.30g$ s
PGV	✓			✓	20 cm/s
I_A	✓		✓	✓	0.4 m/s
I	✓		✓		30 cm/s$^{0.75}$
a_{rms}	✓	✓	✓		0.5 m/s^2

The CAV has been found to correlate well with structural damage potential. The definition of CAV is given by

$$\mathrm{CAV} = \int_0^{t_r} |a_g(t)|\, \mathrm{d}t, \tag{1}$$

where t_r is the total duration of the acceleration trace. The threshold of $0.30g$ s for CAV, obtained after filtering out frequencies above 10 Hz, has been proposed by Benjamin and associates [45], as characterizing intensity greater than VII, contrary to the other criteria that refer to intensity greater than VIII.

The *peak ground velocity* (PGV) is obtained by direct integration of the acceleration trace, which makes it sensitive to the noise content of the accelerogram. For structures with fundamental frequency in the intermediate range, e.g., medium height buildings, and relatively long

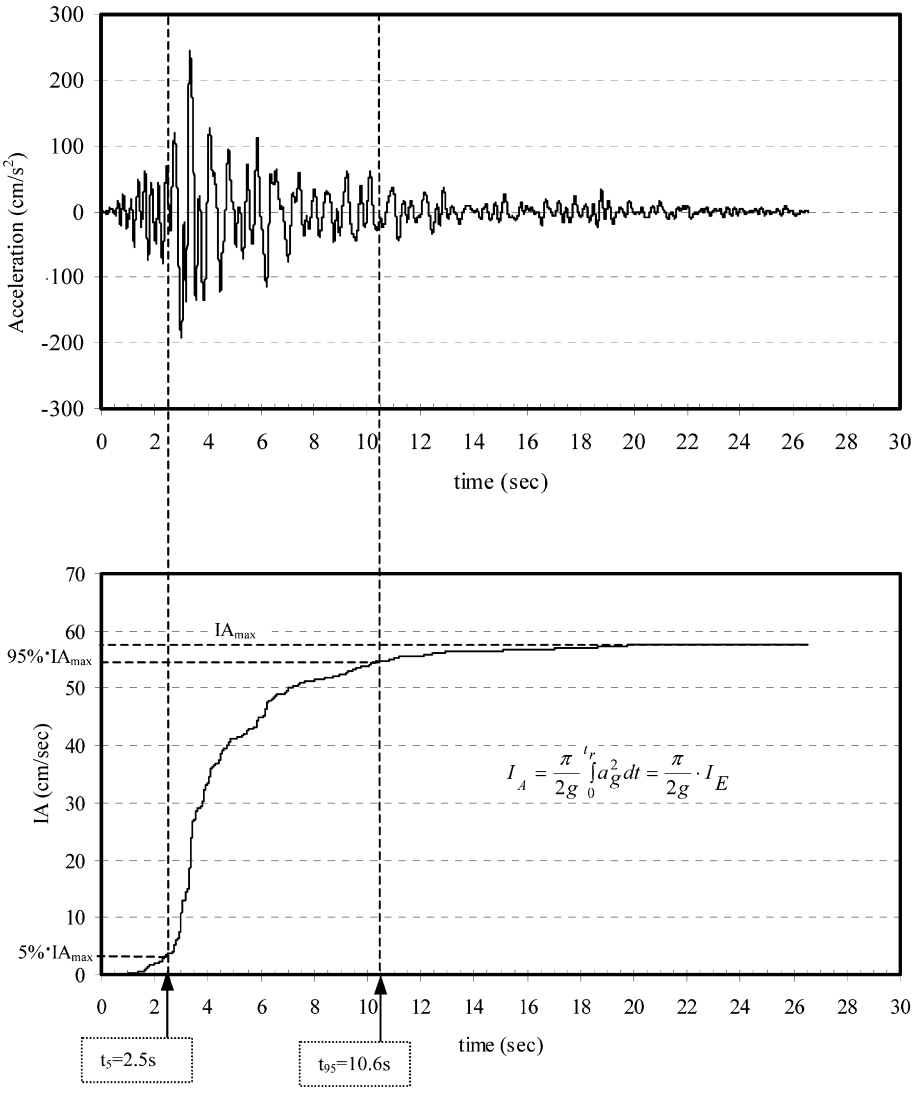

Fig. 2. Husid plot for the transverse component of Lefkas Earthquake of November 4, 1973.

span bridges, PGV is a better indicator of damage potential than PGA [3,32,46]. The PGV in the near-fault region has been found to vary significantly with the magnitude of the seismic event with lower values reported as the distance from the source increases [23].

The *Arias intensity* (I_A) has been proposed as a measure of earthquake intensity [33]. Although, recently, a new empirical relationship has been proposed to estimate Arias intensity [47], the definition valid for small values of damping ratios is used in this study [33]:

$$I_A = \frac{\pi}{2g}\int_0^{t_r} a_g^2 \, dt = \frac{\pi}{2g} I_E, \tag{2}$$

where $a_g(t)$, is the ground acceleration and I_E the integral of the squared ground acceleration.

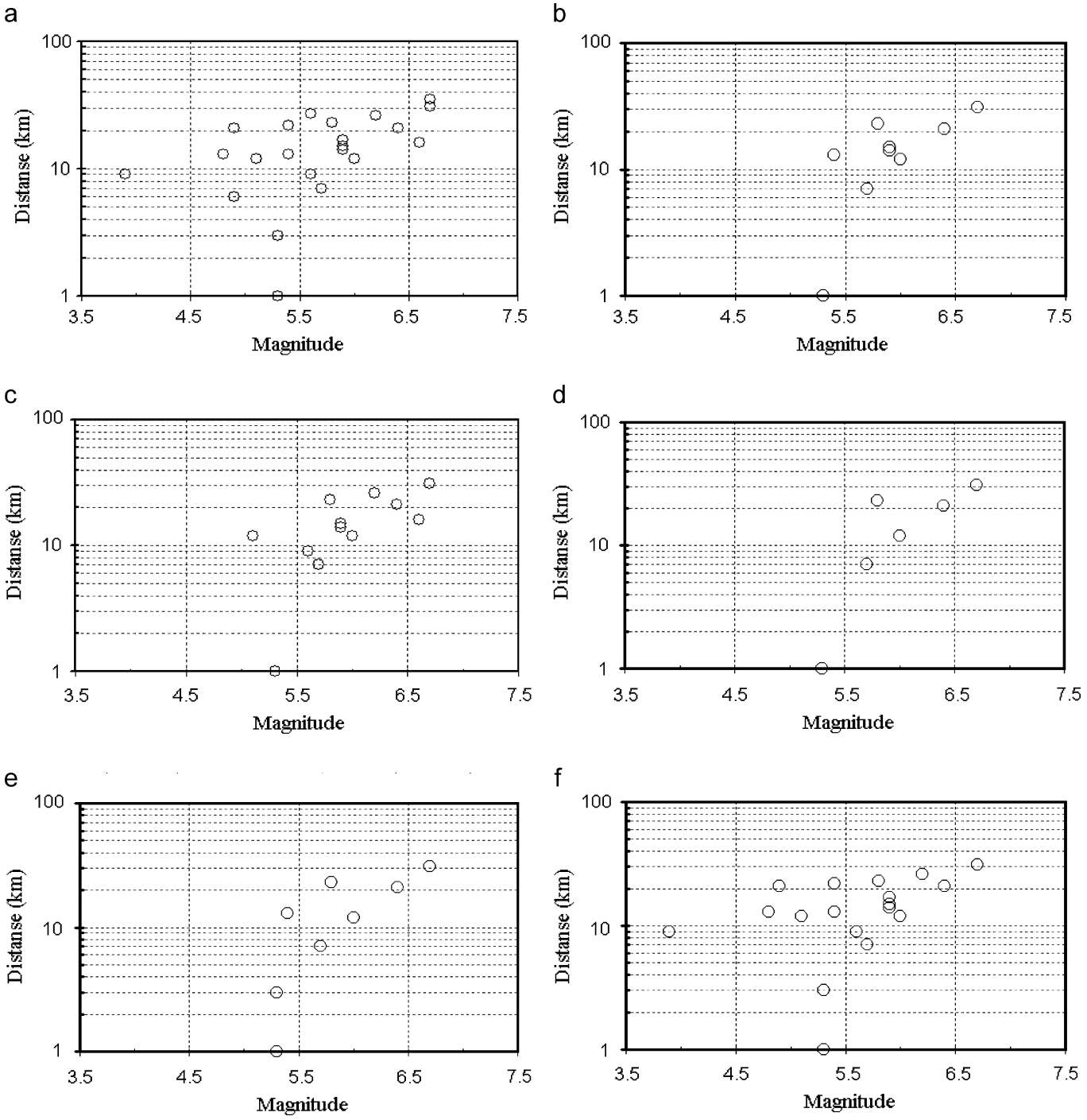

Fig. 3. Application of the near-source identification criteria: (a) 37 records with PGA$\geqslant$0.2g, (b) 21 records with PGA$\geqslant$0.2g and CAV$\geqslant$0.30g s, (c) 16 records with PGA$\geqslant$0.2g and PGV$\geqslant$20 cm/s, (d) 17 records with PGA$\geqslant$0.2g and $I_A\geqslant$0.4 m/s, (e) 13 records with PGA$\geqslant$0.2g and $I\geqslant$30 cm/s$^{0.75}$, (f) 30 records with PGA$\geqslant$0.2g and $a_{rms}\geqslant$0.5 m/s^2.

Fajfar et al. [43] has proposed an empirical damage index (I) intended for medium-period structures. The index incorporates the effects of strong motion duration on the response of medium-rise buildings, and is defined as

$$I = \mathrm{PGV} t_{\mathrm{D}}^{0.25}, \tag{3}$$

where t_{D} is the duration of strong motion. According to Trifunac and Brady [48], t_{D} is defined as the difference between t_5 and t_{95}: t_5 and t_{95} are the start and end of the strong phase of the motion, where 5% and 95% of the total integral of Arias intensity is accumulated, respectively.

The *root mean square acceleration* (a_{rms}) is a single parameter that accounts for the effects of amplitude and frequency content of a strong-motion record and is defined as

$$a_{\mathrm{rms}} = \sqrt{\frac{1}{t_{95}-t_5}\int_{t_5}^{t_{95}} a_{\mathrm{g}}^2(t)\ \mathrm{d}t} = \sqrt{\frac{1}{t_D}\int_{t_5}^{t_{95}} a_{\mathrm{g}}^2(t)\ \mathrm{d}t}. \tag{4}$$

This index is directly proportional to the square root of the gradient of the specified interval of the graph of Arias Intensity versus time, known as the Husid plot [49] and shown in Fig. 2. The lower bound proposed for ground motion intensities MMI = VIII is a_{rms} equal to 0.5 m/s^2 [31].

Table 2 lists the lower bounds for the above parameters that serve as criteria to identify records that correspond to seismic intensities MMI ⩾ VIII.

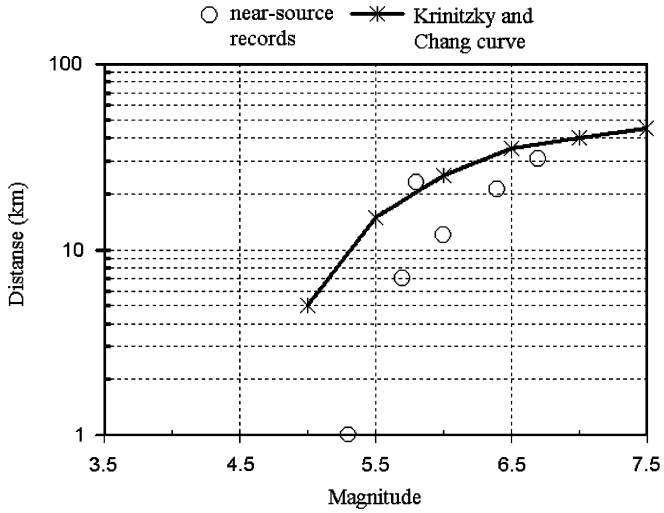

Fig. 4. Eleven records satisfying all the criteria and Krinitzky and Chang's definition for the near source space.

4. Implementation of the criteria and evaluation of the Greek Seismic Code

The first criterion of PGA > 0.2g is satisfied by 37 earthquake record components as shown in Fig. 3(a). Figs. 3(b)–(f), combine the PGA > 0.2g criterion with one more of the other criteria listed in Table 2. Specifically, Fig. 3(b) combines PGA ⩾ 0.2g and CAV ⩾ 0.30g s, Fig. 3(c) combines PGA ⩾ 0.2g and PGV ⩾ 20 cm/s, Fig. 3(d) combines PGA ⩾ 0.2g and I_{A} ⩾ 0.4 m/s, Fig. 3(e) combines PGA ⩾ 0.2g and I ⩾ 30 cm/s$^{0.75}$ and Fig. 3(f) combines PGA ⩾ 0.2g and a_{rms} ⩾ 0.5 m/s^2. Fig. 4 presents the results of the simultaneous application of all criteria. Comparing Fig. 4 with Fig. 3(e), it is observed that the most effective combination of criteria is the simultaneous satisfaction of PGA and the damage potential parameter proposed by Fajfar et al. [43]. As shown in Fig. 4, the space defined from the lower limits of the strong motion parameters is very similar to that defined by Krinitzky and Chang [27]. Notice that earthquakes with magnitude less than M_{w} 4.5 are not considered to develop near-source

Table 3
List of near-source records from earthquakes in Greece

Rec. no.	Seismic event	Date	Fault mechanism	Magnitude (M_{w})	Record	Component	Hypocentral distance (km)	Depth (km)	PVGA/ PHGA
1	Lefkas	11/04/73	RN	$M_{\mathrm{w}} = 5.8$	LEFA7301	L	23 (11)*	20.2	0.265
2						T	23 (11)*	20.2	0.555
3	Korinthos	02/24/81	N	$M_{\mathrm{w}} = 6.7$	KORA8101	L	31 (10)*	10.0	0.477
4				$M_{\mathrm{w}} = 6.7$	XLCA8104	L	31 (8)*	10.0	0.656
5	Kalamata	09/13/86	N	$M_{\mathrm{w}} = 6.0$	KAL18601	L	12 (0)*	0.6	0.826
6				$M_{\mathrm{w}} = 6.0$	KALA8601	T	12 (0)*	0.6	0.718
7						L	12 (0)*	0.6	1.512
8	Kalamata	09/15/86	N	$M_{\mathrm{w}} = 5.3$	KALA8606	L	1 (0)*	8.0	0.532
9	Aegion	06/15/95	N	$M_{\mathrm{w}} = 6.4$	AIGA9501	L	21 (6)**	17.6	0.385
10						T	21 (6)**	17.6	0.367
11	Konitsa	08/09/96	N	$M_{\mathrm{w}} = 5.7$	KON29601	T	7	2.0	0.487

N, normal fault; RN, reverse fault; PVGA: peak vertical ground acceleration.
*fault distance, from Ref. [50].
**normal distance from fault plane, from Ref. [12].

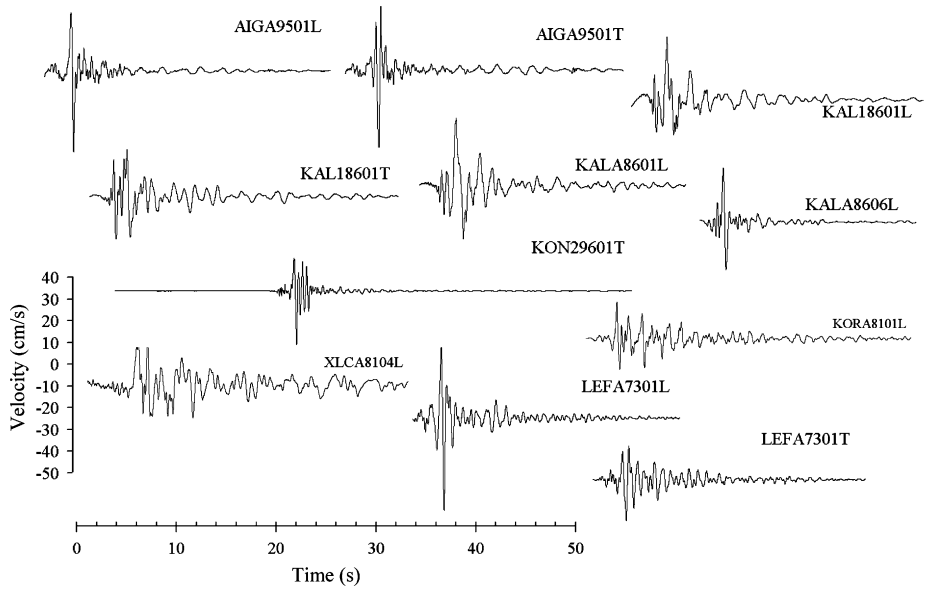

Fig. 5. Strong ground motion velocity traces of the Greek near-source records.

phenomena of engineering interest, a fact that is acknowledged in the literature [31].

The eleven records that satisfy all the criteria belong to the earthquakes that are listed in Table 3, and their velocity traces are shown in Fig. 5. Among the records that satisfy all the imposed criteria are the two accelerograms from the Korinthos 1981 earthquake, obtained at 31 km hypocentral distance. According to the Krinitzky and Chang criteria shown in Fig. 4 the accelerograms from the Korinthos 1981 earthquake ($M_w = 6.7$) could be included in the near-source region although they are recorded at greater distances than usually accepted. This study uses hypocentral distances in order to make a comparison with the definition of near-fault given by Krinitzky and Chang. The two records of Korinthos 1981 earthquake could be considered as near-source since, their fault distance is about 10 km according to reference [50] as shown on Table 3. For the Kalamata 1986 and Aegion 1995 earthquakes the presence of the directivity effect has been confirmed by the spatial distribution of damage [51]. Furthermore it has been ascertained that the impulsive shape of the velocity trace of the Aegion 1995 earthquake record given on lines 9 and 10 of Table 3 has not been induced by amplification of the ground motion caused by local soil conditions [51].

The hypocentral depths for the earthquakes listed in Table 3 are less than 20 km with soil conditions at the recording site characterized as soil type C and D according to EAK 2000. With the exception of the records of the Lefkas 1973 earthquake, all the other records have been corrected with the band-pass filters shown in Fig. 6. The selected transfer function $\tilde{H}(f)$ is given by

$$\tilde{H}(f) = \begin{cases} 0, & 0 < |f| < f_1, \\ 1, & f_2 < |f| < f_3, \\ 0, & f_4 < |f|. \end{cases} \quad (5)$$

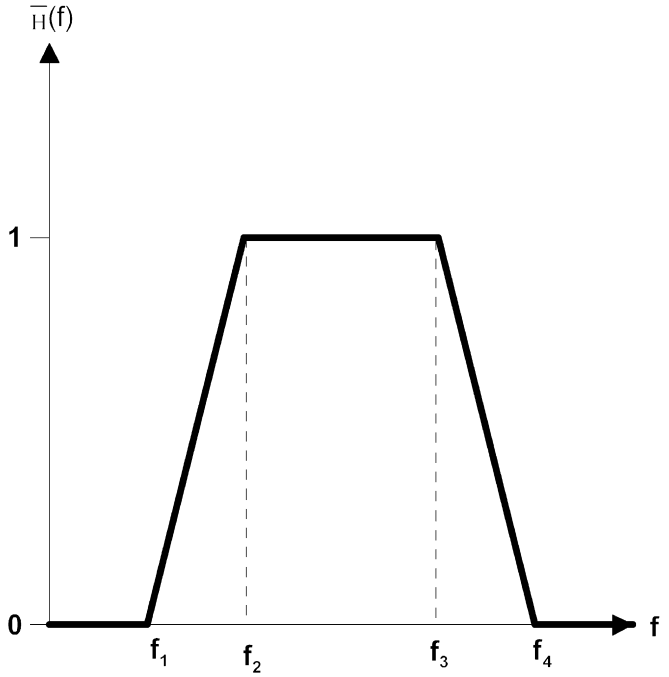

Fig. 6. Band-pass filtering applied to Greek records ($0.075 < f_1 < 0.413$ Hz, $0.125 < f_2 < 0.572$ Hz, $f_3 = 25$ and $f_4 = 27$ Hz).

The frequency f_1 varies between 0.075 and 0.413 Hz, f_2 varies between 0.125 and 0.572 Hz, f_3 and f_4 are selected as equal to 25 and 27 Hz, respectively [35,36]. For the international records the filters are specified in [37–39].

In order to examine the adequacy of EAK 2000 [40] to account for near-source effects, two records are selected and their pseudo-acceleration spectra for 5% damping are compared with the corresponding linear elastic spectra of EAK 2000. The first record is the longitudinal component of the Lefkas earthquake of November 4, 1973 on soil type D according to the EAK 2000 soil classification, that

occurred in seismic hazard zone with maximum ground acceleration equal to $0.36g$ having a 10% probability of exceedance in 50 years. The second record refers to the transverse component of Aegion earthquake of June 15, 1995 on soil type C according to the EAK 2000 soil classification, that occurred in seismic hazard zone with maximum ground acceleration equal to $0.24g$ having a 10% probability of exceedance in 50 years. The results are shown in Fig. 7, where the elastic response spectra for 5% damping of Lefkas and Aegion are compared with spectra defined by EAK 2000 [40] for the soil type C and D either for far-fault or for the near-fault region. In the later case the spectra have been increased by 25%. Notice that the increase of 25% specified by EAK 2000 for structures located near an active fault is not conservative for $T<0.75$ s. Certainly, comparison of two representative near-source records is not sufficient to arrive at definite conclusions and recommendations; however, it highlights the need to examine the issue in more detail.

Besides certain possible modifications of the Greek seismic code, it is also of interest to investigate whether near-source ground motion with damaging potential can be correlated with a certain type of ground acceleration, velocity or displacement pulse, an issue that is examined in the following section.

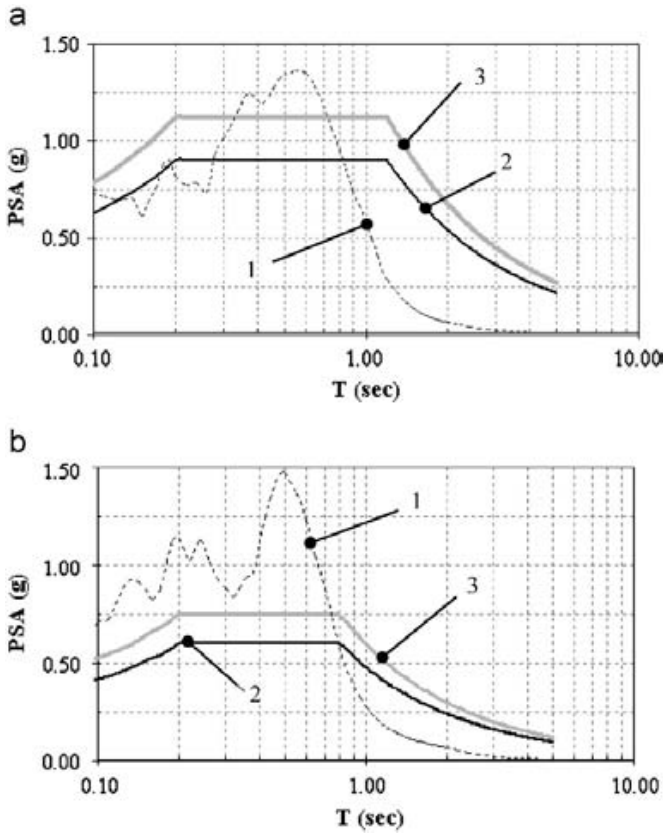

Fig. 7. Near-source PSA spectra and corresponding elastic spectra of EAK 2000: (a) (1) Lefkas (1973) longitudinal component PSA spectrum, (2) EAK 2000 spectrum and (3) EAK 2000 spectrum increased by 1.25; (b) (1) Aegion (1995) transverse component PSA spectrum, (2) EAK 2000 spectrum and (3) EAK 2000 spectrum increased by 1.25.

5. Impulse type classification for near-source ground motions

The effect of near-source ground excitations on earthquake design has been associated with characteristics of the impulsive nature of this kind of motion [7]. In the literature, there is a substantial number of simplified representations, used mostly in seismology, in the form of "pulse" shapes that attempt to capture the salient features of near-source ground motions, e.g., Mavroeidis and Papageorgiou [12]. Most representations are based on wavelets used by seismologists independently from the distance from the source, e.g., Gabor [10] and the generalized Rayleigh wavelet mentioned in Hudson [11]. These wavelets utilize four parameters to determine the waveform characteristics of the near-source velocity pulses, that is, the amplitude, the prevailing frequency (or prevailing period), the phase of the wavelet and the oscillatory character. Some researchers, such as Ricker [9] utilize two parameters, that is, amplitude and prevailing frequency.

In the present study the velocity pulses are distinguished as the type-A, type-B and type-C_n shown in Figs. 8(a)–(c), respectively. The equations that govern the type-A pulse are the following [5]:

$$
\begin{aligned}
a_g^A &= \omega_p \frac{v_p}{2}\sin(\omega_p t), \quad 0 \leqslant t \leqslant T_p,\\
v_g^A &= \frac{v_p}{2} - \frac{v_p}{2}\cos(\omega_p t), \quad 0 \leqslant t \leqslant T_p,\\
d_g^A &= \frac{v_p}{2} t - \frac{v_p}{2\omega_p}\sin(\omega_p t), \quad 0 \leqslant t \leqslant T_p,
\end{aligned} \tag{6}
$$

where $\omega_p = 2\pi/T_p$. For type-B the pulse is expressed by

$$
\begin{aligned}
a_g^B &= \omega_p v_p \cos(\omega_p t), \quad 0 \leqslant t \leqslant T_p,\\
v_g^B &= v_p \sin(\omega_p t), \quad 0 \leqslant t \leqslant T_p.
\end{aligned} \tag{7}
$$

For the type-C_n pulse the displacement history exhibits one or more long duration cycles. An $n+$half cycles, or $2n+1$ half-cycles ground displacement, characterized as type-C_n pulse, can be defined by

$$
\begin{aligned}
a_g^C &= \omega_p v_p \cos(\omega_p t + \varphi) \quad 0 \leqslant t \leqslant \left(n + \frac{1}{2} - \frac{\varphi}{\pi}\right) T_p,\\
v_g^C &= v_p \sin(\omega_p t + \varphi) - v_p \sin(\varphi) \quad 0 \leqslant t \leqslant \left(n + \frac{1}{2} - \frac{\varphi}{\pi}\right) T_p,\\
d_g^C &= -\frac{v_p}{\omega_p}\cos(\omega_p t + \varphi) - v_p t \sin(\varphi)\\
&\quad + \frac{v_p}{\omega_p}\cos(\varphi) \quad 0 \leqslant t \leqslant \left(n + \frac{1}{2} - \frac{\varphi}{\pi}\right) T_p,
\end{aligned} \tag{8}
$$

where φ is the phase angle, determined by imposing zero ground displacement at the end of the pulse duration. Type-C_1 pulses are characterized by three half-cycles, while type-C_2 pulses characterized by five half-cycles, as shown in Fig. 8(c).

An evaluation of the eleven records listed in Table 4 revealed that five records present a single dominant velocity pulse and can be characterized as impulsive

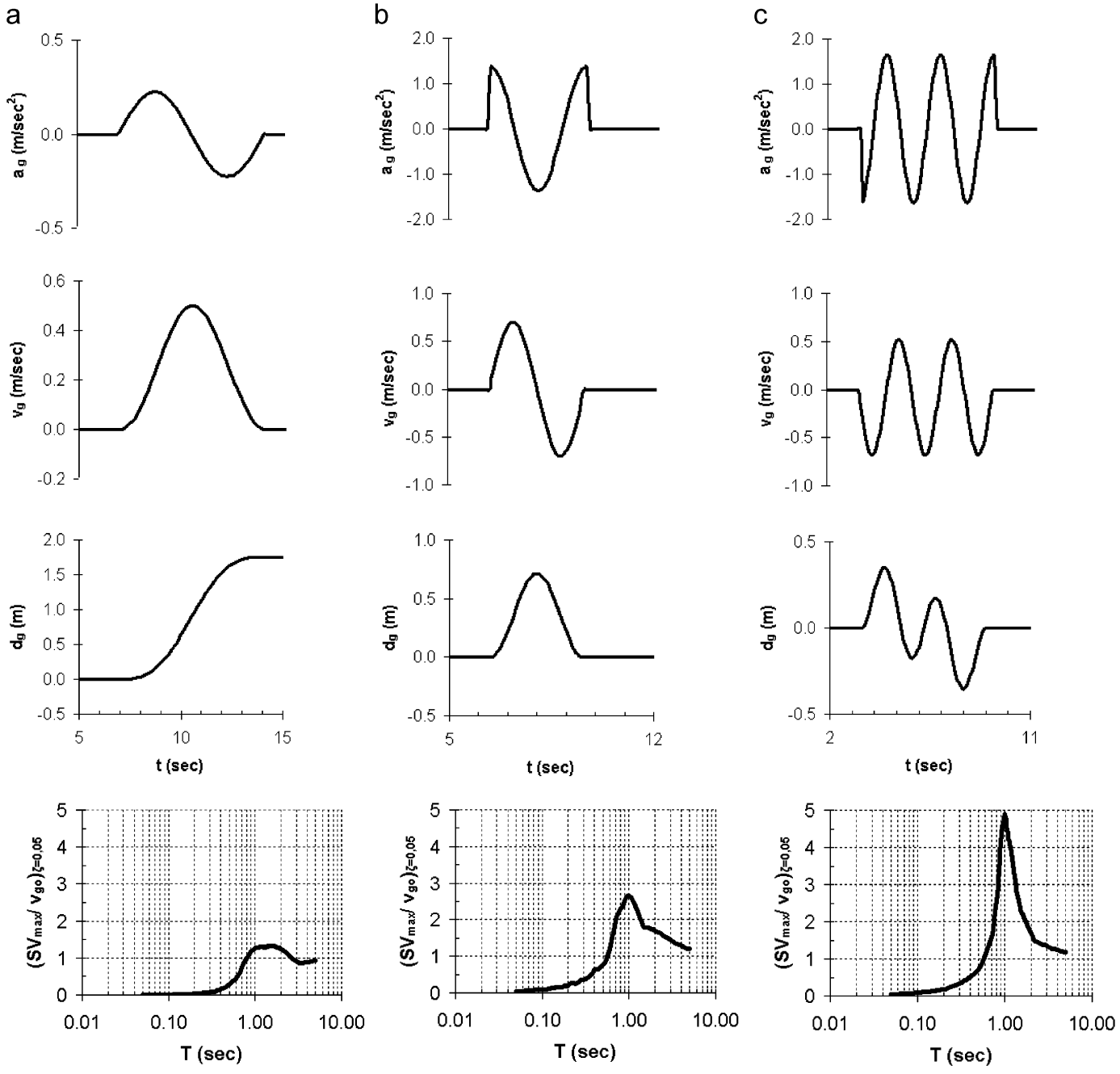

Fig. 8. (a) Pulse type-A, (b) pulse type-B, and (c) pulse type-C_2.

motions of type-B. The other six records can be characterized as type-C_n impulsive motions. It should be noted that type-A impulsive motions that are capable to induce significant MMI intensities have not been identified from the available 860 strong ground-motion records in Greece used in this study.

In order to evaluate and differentiate the impulsive types, the following parameters are calculated:

- The predominant period T_p that corresponds to the maximum spectral velocity (SV) for $\xi = 0.05$, as defined in reference [52]. According to Bray and Rodriguez-Marek [23], T_p is expected to be a function of the moment magnitude, the period of the velocity pulse is related with the duration of the velocity pulse with the largest amplitude, and it is ascertained that lower magnitude earthquakes are expected to have lower pulse periods.
- The maximum ratio of SV to PGV for $\xi = 0.05$ $(SV_{max}/PGV)_{\zeta=0.05}$. The reason to use this normalized index is to facilitate the correlation between the recorded strong motion and the type-A, type-B and C_n pulses.

Table 4
Parameters for the 11 near-source component records

Rec. no.	Record	Comp.	Pulse type	PGA (g)	PGV (cm/s)	PGD (cm)	CAV (g s)	I_A (cm/s)	I (cm/s$^{-0.75}$)	a_{rms} (cm/s^2)	PGV/PGA (s)	PGD/PGV (s)	t_D (s)	$(SV_{max}/v_{go})_{\zeta=0.05}$	T_p (s)
1	LEFA7301	L	B	0.50	45.15	4.48	0.62	130.60	75.02	115.58	0.09	0.10	5.50	2.67	0.70
2		T	C	0.24	20.28	2.15	0.53	57.74	37.95	61.88	0.09	0.11	8.48	3.53	0.75
3	KORA8101	L	C	0.23	22.98	3.43	0.70	66.21	43.08	53.01	0.10	0.15	13.25	3.24	0.80
4	XLCA8104	L	C	0.30	26.26	9.43	0.88	90.01	49.36	58.16	0.09	0.36	14.96	3.11	1.00
5	KAL18601 KALA8601	L	C	0.23	29.91	5.32	0.45	51.34	31.54	78.44	0.13	0.18	4.69	3.19	0.65
6		T	C	0.27	23.93	5.30	0.54	75.72	36.45	86.60	0.09	0.22	5.68	3.16	0.70
7		L	C	0.22	32.81	7.33	0.52	54.66	33.59	74.64	0.15	0.22	5.52	3.13	1.15
8	KALA8606	L	B	0.33	26.28	4.17	0.30	52.14	31.99	116.21	0.08	0.16	2.17	2.95	0.65
9	AIGA9501	L	B	0.49	43.54	6.20	0.49	98.37	57.53	136.56	0.09	0.14	2.97	2.19	0.65
10		T	B	0.52	43.01	4.53	0.51	115.92	50.68	179.82	0.08	0.11	2.02	2.79	0.55
11	KON29601	T	B	0.39	25.90	2.57	0.36	60.79	31.08	120.07	0.07	0.10	2.37	2.87	0.40

The number of half-sine cycles in the velocity time history has been related with the fault characteristics and the fault slip distribution [15,23].

Table 4 presents the results for all the parameters calculated for the eleven near-source records. The ratio $(SV_{max}/v_{go})_{\zeta=0.05}$ is also calculated for the simple theoretical pulses and plotted in Fig. 11(a). Notice that records of the same earthquake that are obtained at the same hypocentral distance have practically the same value of the SV_{max}/v_{go} ratio, independently of the direction. This similarity is observed, for example, in the Korinthos 1981 and Kalamata 1986 mainshock records, as shown in Fig. 11(a). The Greek near-source velocity pulses seem to belong to one or one and a half sinusoidal impulsive motion, that is type-B and type-C_1 pulses, respectively. The type-A pulses represented by the continuous line in Fig. 11(a) appear to have the smallest values of the SV_{max}/v_{go} ratio. Even though velocity records with an SV_{max}/v_{go} ratio of about 1.3, which characterizes type-A pulses, are not found, it cannot be excluded that type-A velocity pulses may be identified in the future. It is also possible that type-A velocity pulses have occurred but have either not been recorded or have been distorted by filtering procedures. However, significant permanent displacement phenomena induced by Greek earthquakes that are related with type-A velocity pulses have not been reported in Ref. [53]. The absence of this type of pulse is possibly related to the fault characteristics of the Greek region. The role of the type of fault mechanism in affecting the shape and the direction of the predominant pulse is acknowledged in Ref. [54]. In the Greek region, which is characterized by dip-slip faulting, a combination of directivity-pulse and fling-step is expected to take place in a horizontal direction [54]. No permanent displacements in the order of the Chi-Chi and Kocaeli 1999 earthquakes have been recorded, so far. Also, records from significant and catastrophic Greek earthquakes, like the Athens earthquake of September 7, 1999, have not been obtained at relatively small distances from the source [55].

Fig. 11(b) presents the predominant periods T_p of the Greek records as related to magnitude, while the relation of the PGV with the earthquake magnitude and distance from the source is presented in Fig. 11(c). Notice that PGV varies from 20 to 45 cm/s for the Greek records. Since all the T_p values are between 0.4 and 1.15 s (0.87–2.5 Hz), it is expected that the filters used for processing have not distorted the significant part of the strong motion, since the predominant frequency varies between the f_2 and f_3 frequencies specified in Section 4.

6. Comparison with international near-source records

The characteristics of the Greek near-source earthquake records are compared with several accelerograms of international seismic events recorded in the near-source region. Table 5 lists representative near-fault records from

Table 5
Strong motion data set of near-source international earthquake records

No	Earthquake	Date	Fault mechanisms	Magnitude (M_w)	Station	Component	Distance (km)	PVGA/ PHGA
1	Parkfield	06/28/66	SS	6.1	Cholame #2	CO2065	R_{jb} 6.60	0.536
2	Tabas	09/16/78	RN	7.4	Tabas	TAB-TR	R_{hyp} 3.00	0.808
3	Imperial Valley	10/15/79	SS	6.5	El Centro Array #5	H-E05230	R_{jb} 4.00	1.417
4				6.5	El Centro Array #6	H-E06230	R_{jb} 1.30	3.770
5				6.5	Meloland	H-EMO270	R_{jb} 0.50	0.838
6	Loma Prieta	10/18/89	RO	6.9	16 LGPC	LGP000	R_{wp} 6.10	1.581
7	Landers	06/28/92	SS	7.3	Lucerne	LCN275	R_{wp} 1.10	1.134
8	Northridge	01/17/94	RN	6.7	Jensen Filter Plant	JEN022	R_{wp} 6.20	0.943
9				6.7	Rinaldi Receiving	RRS228	R_{wp} 7.10	1.017
10				6.7	Sylmar–Converter	SCS052	R_{wp} 6.20	0.958
11				6.7	Sylmar–Olive View Med FF	SYL360	R_{wp} 6.40	0.635
12	Kobe	01/16/95	SS	6.9	Takatori	TAK000	R_{wp} 0.30	0.445
13	Chi-Chi	09/20/99	RN	7.6	TCU068	TCU068	R_{wp} 1.09	1.052
14	Kocaeli	07/17/99	SS	7.4	Sakarya	SKR090	R_{wp} 3.10	0.689
15	Nicaragua	12/23/72		6.2	Esso Refinery	nic02_060_E	R_{epi} 16.00	0.850
16					Esso Refinery	nic02_058_S		0.939
17	San Salvador	10/10/86		5.7	Geo. Inv. center	Sal01_005_90	R_{epi} 4.00	0.560
18					Geo. Inv. center	Sal01_005_180		0.926
19	Yountville	09/03/00		5.0	Napa, CA	2016a_v90	R_{hyp} 9.80	1.253
20					Napa, CA	2016b_360		1.010

SS, strike slip fault; RN, reverse faul; RO, reverse-oblique fault; R_{wp}, closest to fault rupture; R_{jb}, closest to surface projection of rupture; R_{hyp}, hypocentral R_{epi}: epicentral; PVGA, peak vertical ground acceleration; PHGA, peak horizontal ground acceleration.

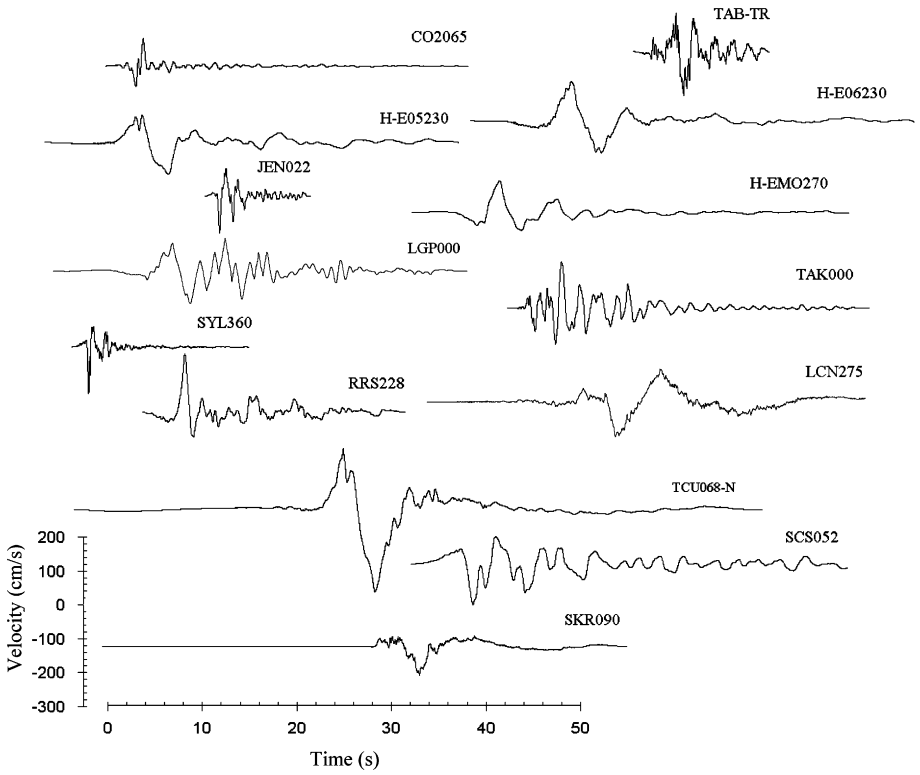

Fig. 9. Strong ground-motion velocity traces of international near-source records.

the Parkfield (1966), Tabas (1978), Imperial Valley (1979), Loma Prieta (1989), Landers (1992), Northridge (1994), Kobe (1995), Chi-Chi (1999) and Kocaeli (1999) earthquakes. These records correspond to great and large earthquakes and have strong impulsive character in their velocity traces, as shown in Fig. 9. The ground

Table 6
Pulse type characterazation and ground motion parameters of near-source international earthquake records

Rec. no.	Record	Component	Pulse type	PGA (g)	PGV (cm/s)	PGD (cm)	CAV (g s)	I_A (cm/s)	I (cm/s$^{0.75}$)	a_{rms} (cm/s^2)	PGV/ PGA (s)	PGD/ PGV (s)	t_D (s)	(SV_{max}/v_{go}) $\zeta = 0.05$	T_p (s)
1	Parkfield	CO2065	B	0.476	75.1	22.49	0.90	319.89	122.11	160.38	0.16	0.30	6.99	1.95	1.80
2	Tabas	TAB-TR	C	0.852	121.4	94.58	0.90	1153.10	243.25	200.52	0.15	0.78	16.12	2.74	4.70
3	Imp. Valley	H-E05230	B	0.379	90.5	63.03	0.95	178.26	158.51	103.19	0.24	0.70	9.41	2.33	3.50
4	Imp. Valley	H-E06230	B	0.439	109.8	65.89	0.99	175.40	187.43	107.76	0.25	0.60	8.49	2.29	3.30
5	Imp. Valley	H-EMO270	C	0.296	90.5	31.71	0.77	107.96	145.87	94.82	0.31	0.35	6.75	2.26	3.10
6	Loma Prieta	LGP000	C	0.563	94.8	41.18	1.79	786.54	169.33	208.39	0.17	0.43	10.18	2.71	3.20
7	Landers	LCN275	B	0.721	97.6	70.31	1.73	695.17	185.70	172.67	0.14	0.72	13.11	2.37	4.20
8	Northridge	JEN022	C	0.424	106.2	43.06	0.95	264.93	199.29	109.58	0.26	0.41	12.40	2.37	2.80
9		RRS228	C	0.838	166.1	28.78	1.65	737.07	270.46	242.76	0.20	0.17	7.03	1.80	1.00
10		SCS052	C	0.612	117.4	53.47	2.07	583.10	231.39	147.37	0.20	0.46	15.09	2.57	2.85
11		SYL360	B	0.843	129.6	32.68	1.73	501.23	196.83	230.12	0.16	0.25	5.32	1.67	2.60
12	Kobe	TAK000	C	0.611	127.1	35.77	2.64	869.65	233.24	207.62	0.21	0.28	11.34	3.03	2.10
13	Chi-Chi	TCU068-N	B	0.462	263.1	430.00	1.79	165.71	499.92	84.53	0.58	1.63	13.04	1.81	8.00
14	Kocaeli	SKR090	B	0.376	79.5	70.52	0.93	175.82	140.88	100.11	0.22	0.89	9.86	1.48	5.70
15	Nicaragua	nic02_060_E	C	0.358	35.1	13.80	1.07	157.96	63.72	90.42	0.10	0.39	10.86	2.14	0.90
16		nic02_058_S	C	0.324	30.3	6.30	1.09	200.26	51.37	116.74	0.10	0.21	8.26	3.21	0.42
17	San Salvador	Sal01_005_90	B	0.694	80.0	11.90	0.73	248.57	115.26	180.26	0.12	0.15	4.30	1.80	0.85
18		Sal01_005_180	B	0.420	61.8	14.80	0.58	168.46	81.90	175.34	0.15	0.24	3.08	2.58	0.70
19	Yountville	2016a_v90	B	0.409	39.7	4.22	0.55	109.12	52.49	142.16	0.10	0.11	3.04	2.59	0.65
20		2016b_360	C	0.508	34.2	2.47	0.53	102.54	46.51	130.10	0.07	0.07	3.41	2.34	0.75

accelerations range between 0.296 and 0.852g. The same parameters used for the records of the Greek region are evaluated for the international records and presented in Table 6. Tables 5 and 6 include records of small-to-moderate earthquakes with near-source effects, that is from the Nicaragua (1972), San Salvador (1986) and Yountville, CA (2000) earthquakes [24]. The corresponding velocity traces are presented in Fig. 10.

All records satisfy the criteria listed in Table 2, so they can be characterized as near-source. The great majority of the predominant periods of great and large earthquakes varies between 2 and 8 s, as listed in Table 6, and are clearly greater than the period of the Greek pulses shown in Fig. 5. It is observed that the predominant period of the pulse tends to increase with magnitude, a fact that agrees with the study of Bray and Rodriguez-Marek [23]. From Figs. 11(c) and 12(c) notice that PGV increases with magnitude and decreases with distance. The $(SV_{max}/v_{go})_{\zeta=0.05}$ ratio is calculated for the international records and plotted in Fig. 12(a). As shown in Fig. 12(a) velocity traces with prominent type-A pulse, like the Chi-Chi and Kocaeli records, present the smallest amplification of SV.

The diagrams for the Greek records in Figs. 11(b) and (c) include only the records of small-to-moderate magnitude international earthquakes, such as the San Salvador 1986 earthquake, that seem to have about the same T_p as the Greek records. Since T_p varies between 0.4 and 1.15 s as shown in Fig. 11(b), medium period structures with fundamental period less than 1 s at sites located close to active faults may be subjected to a more damaging motion for earthquakes of lower magnitude. Medium-rise buildings, common to urban areas, with fundamental periods near the predominant period of the velocity pulse induced by a small-to-moderate earthquake, are expected to experience larger earthquake demand than the one caused by seismic events of greater magnitude [23,24].

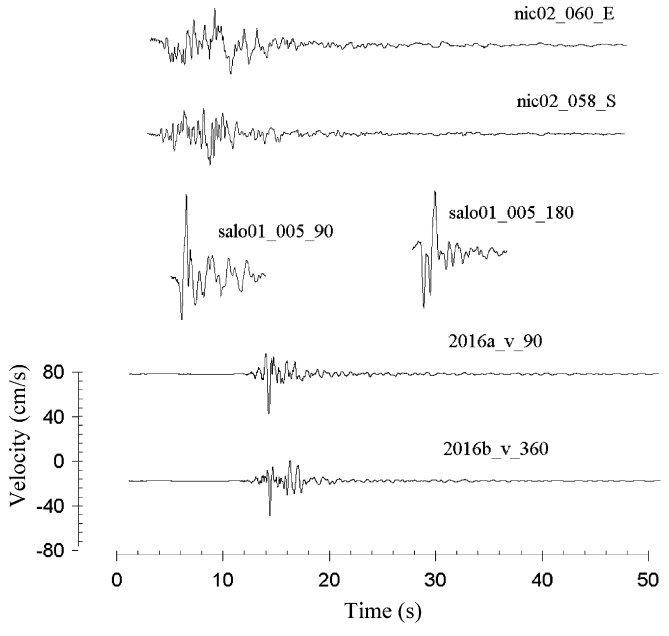

Fig. 10. Strong ground-motion velocity traces of international near-source records with small-to-moderate magnitude.

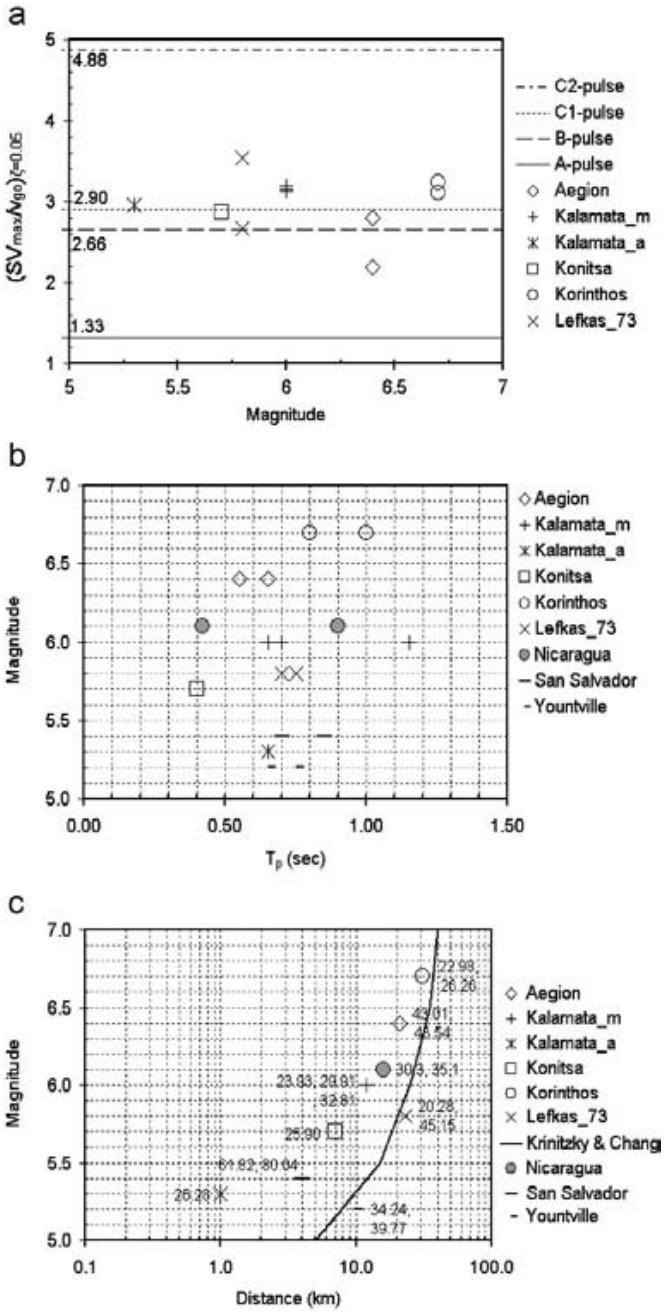

Fig. 11. Impulsive motion parameters of Greek and small-to-moderate international earthquakes: (a) $(SV_{max}/PGV)_{\zeta=0.05}$ versus magnitude, (b) magnitude versus T_p, (c) PGV for distance from the source versus magnitude.

7. Conclusions

This work studies the majority of the available accelerograms of the Greek region, recorded from 1973 to 1999, which are characterized by relatively small-to-moderate earthquake magnitudes, in order to identify near-source characteristics. Six criteria that relate several

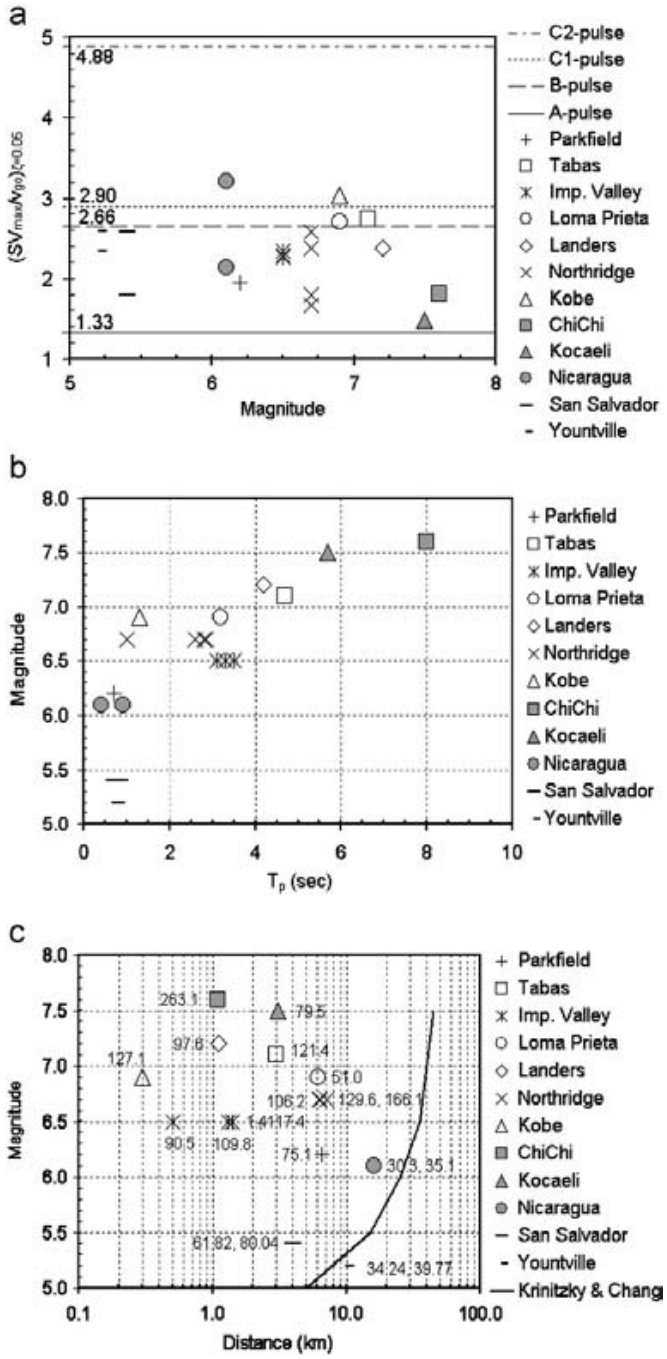

Fig. 12. Impulsive motion parameters of international earthquakes: (a) $(SV_{max}/PGV)_{\zeta=0.05}$ versus magnitude, (b) magnitude versus T_p, (c) PGV for distance from the source versus magnitude.

parameters of ground motion are used to identify records capable causing intensities greater than VII or VIII on the Modified Mercalli scale (MMI). Furthermore, the distance to magnitude M_w relation of the records is compared with definitions for the near-source given in the literature.

The study also presents a comparison between Greek records and well-known international near-source records from small, moderate and strong earthquakes. The predominant period of the velocity pulse, T_p, and the maximum ratio of SV to PGV, $(SV_{max}/PGV)_{\xi=0.05}$, are calculated and compared with the corresponding values of the international near-source records and simple wavelets.

The research has led to the following conclusions:

(a) The most effective combination of criteria in defining the near-source region is found to be the combination of peak ground acceleration, $PGA \geqslant 0.20g$ and the damage potential parameter proposed by Fajfar, $I \geqslant 30\,cm/s^{0.75}$, since it includes the majority of the records obtained by the simultaneous satisfaction of all criteria.

(b) Since the records identified by the parametric study of the Greek strong-motion databases are obtained in regions in which directivity phenomena have occurred, there is a strong indication that the damage criteria can be successfully used to identify records with near-source characteristics.

(c) Selected near-source records are found to exceed the demand specified by the corresponding elastic spectra of the current Greek Seismic Code. This observation supports the argument that further research is needed in order to arrive at results and procedures applicable to earthquake design in regions with small-to-moderate earthquakes, such as Greece.

(d) The applicability of the Krinitzky and Chang [27] definition for the near-source region for both small and large magnitude earthquakes is confirmed. Near-source records of small-to-moderate magnitude belong to the upper bound of the near-source region and are characterized by velocity pulses of significantly smaller T_p and PGV than records of greater earthquake magnitude. This difference is more obvious for earthquake magnitudes $M_w > 6.5$ and records obtained at distance less than 7 km from the fault, where the larger values of T_p and PGV are recorded, as shown in Figs. 12(b) and (c).

(e) The opinion that earthquakes of magnitude smaller than M 6.0 could present near-source characteristics is strengthened. The possibility of severe damage potential to be related with near-source characteristics (forward directivity, polarization) in earthquakes of small-to-moderate magnitude necessitates their inclusion in earthquake engineering design and urges for further research related to near-source effects on medium-period structures, which seem to be threatened mostly by small-to-moderate earthquakes.

(f) The ratio of SV to PGV for a damping ratio $\zeta = 5\%$ is found to be a good indicator of the velocity pulse type. According to this criterion two or three half-cycles characterize the Greek records velocity traces, classifying them as type-B and type-C_1 pulse types. It is found that pulse type-A related with permanent displacement phenomena does not characterize the existing Greek records.

Acknowledgments

The authors are grateful to the Institute of Engineering Seismology and Earthquake Engineering (ITSAK) and the Geodynamic Institute of the National Observatory of Athens that kindly provided the accelerograms. The research of Ch.A. Maniatakis is funded by a doctoral scholarship from Alexander S. Onassis Public Benefit Foundation. This financial support is gratefully acknowledged.

References

[1] Housner GW, Trifunac MD. Analysis of accelerograms: Parkfield earthquake. Bull Seismol Soc Am 1967;57:1193–220.
[2] Boore DM, Zoback MD. Two dimensional kinematic fault modeling of the Pacoima Dam strong motion records of February 9, 1991, San Fernando earthquake. Bull Seismol Soc Am 1974;64:555–70.
[3] Bertero VV, Mahin SA, Herrera RA. Aseismic design implications of near-fault San Fernando earthquake records. Eathquake Eng Struct Dyn 1978;6:31–42.
[4] Naeim F. On seismic design implications of the 1994 Northridge earthquake record. Earthquake Spectra 1995;11(1):91–109.
[5] Makris N. Rigidity-plasticity-viscocity: can electrorheological dampers protect base-isolated structures from near-source ground motions. Earthquake Eng Struct Dyn 1997;26:571–91.
[6] Chopra AK, Chintanapakdee C. Comparing response of SDF systems to near-fault and far-fault earthquake motions in the context of spectral regions. Earthquake Eng Struct Dyn 2001;30:1769–89.
[7] Mavroeidis GP, Dong G, Papageorgiou AS. Near-fault ground motions, and the response of elastic and inelastic single-degree-of-freedom (SDOF) systems. Earthquake Eng Struct Dyn 2004;33:1023–49.
[8] Ambraseys NN, Bommer JJ. The attenuation of ground accelerations in Europe. Earthquake Eng Struct Dyn 1991;20:1179–202.
[9] Ricker N. Wavelet contraction, wavelet expansion, and the control of seismic resolution. Geophysics 1953;18:769–92.
[10] Gabor D. Theory of communication. I. The analysis of information. IEEE 1946;93:429–41.
[11] Hudson JA. The excitation and propagation of elastic waves. Cambridge, MA: Cambridge University Press; 1980.
[12] Mavroeidis G, Papageorgiou A. A mathematical representation of near-fault ground motions. Bull Seismol Soc Am 2003;93(3):1099–131.
[13] Hall JF, Heaton TH, Halling MW, Wald DJ. Near-source ground motion and its effects on flexible buildings. Earthquake Spectra 1995;11(4):569–605.
[14] Elnashai AS, Papazoglou AJ. Procedure and spectra for analysis of RC structures subjected to vertical earthquake loads. J Earthquake Eng 1997;1:121–55.
[15] Somerville PG, Smith NF, Graves RW, Abrahamson NA. Modification of empirical strong ground motion attenuation relations to include the amplitude and duration effects of rupture directivity. Seismol Res Lett 1997;68(1):199–222.
[16] Iwan WD, Chen XD. Important near-field ground motion data from the Landers earthquake. In: Proceedings of the 10th European conference on earthquake engineering, Vienna, 1994.
[17] Boore DM, Bommer JJ. Processing of strong-motion accelerograms: needs, options and consequences. Soil Dyn Earthquake Eng 2005;25(2):93–115.
[18] Rathje EM, Faraj F, Russell S, Bray JD. Empirical relationships for frequency content parameters of earthquake ground motions. Earthquake Spectra 2004;20(1):119–44.
[19] Rathje EM, Abrahamson NA, Bray JD. Simplified frequency content estimates of earthquake ground motions. J Geotech Eng Div ASCE 1998;124(2):150–9.
[20] Bommer JJ, Mendis R. Scaling of spectral displacement ordinates with damping ratios. Earthquake Eng Struct Dyn 2005;34(2):145–65.
[21] Somerville PG. Magnitude scaling of the near fault rupture directivity pulse. Phys Earth Planetary Interiors 2003;137:201–12.
[22] Abrahamson NA. Effects of rupture directivity on probabilistic seismic hazard analysis. In: Proceedings of the 6th international conference on seismic zonation, Earthquake Engineering Research Institute. Palm Springs, 2000.
[23] Bray JD, Rodriguez-Marek A. Characterisation of forward-directivity ground motions in the near-fault region. J Soil Dyn Earthquake Eng 2004;24:815–28.
[24] Bommer JJ, Georgallides G, Tromans IJ. Is there a near-field for small-to-moderate magnitude earthquakes? J Earthquake Eng 2001;5(3):395–423.
[25] Campbell KW. Near-source attenuation of peak horizontal acceleration. Bull Seismol Soc Am 1981;71:2039–70.
[26] Bolt BA, Abrahamson NA. New attenuation relations for peak and expected accelerations of strong ground-motion. Bull Seismol Soc Am 1982;72:2307–21.
[27] Krinitzky EL, Chang FK. State of the art for assessing earthquake hazards in the United States: parameters for specifying intensity related earthquake ground motions. US Army Corps of Engineering Waterways Experiment Station, Report 25, 1987.
[28] Hudson DE. Some recent near-source strong motion accelerograms. In: Proceedings of the ninth world conference on earthquake engineering, vol. 2, Tokyo-Kyoto, 1988.
[29] Ambraseys NN, Menu JM. Earthquake-induced ground displacement in Europe. Earthquake Eng Struct Dyn 1988;16:985–1006.
[30] Bommer JJ. The design and engineering application of an earthquake strong-motion database. Ph.D Thesis, Imperial College, University of London, 1991.
[31] Martinez-Pereira A, Bommer JJ. What is the near-field? In: Seismic design practice into the next century. Rotterdam: Booth editions; 1998. p. 245–52.
[32] Martinez-Pereira A. The characterisation of near-field earthquake ground-motions for engineering design. Ph.D. Thesis, Imperial College, University of London; 1999.
[33] Arias A. A measure of earthquake intensity. In: Hansen RJ, editor. Seismic design for nuclear power plants. Cambridge, MA: MIT Press; 1970. p. 438–83.
[34] Spyrakos CC, Maniatakis ChA, Taflambas J. Critical evaluation of near-field seismic records in Greece. In: Brebbia CA, Beskos DE, Manolis GD, Spyrakos CC, editors. Earthquake resistant engineering structures. WIT Press; 2005. p. 53–62.
[35] Kalogeras IS. Strong motion database. Time period 1973–1999. National Observatory of Athens, Institute of Geodynamics Publication 15 (CD-ROM with user's manual), 2001.
[36] Theodulidis N, Kalogeras I, Papazachos C, Karastathis V, Margaris V, Papaioannou Ch, et al. HEAD v.10: A unified Hellenic Accelerogram Database. Seism Res Lett 2004;75(1):36–45.
[37] PEER Strong Motion Database, 〈http://www.peer.berkeley.edu〉.
[38] COSMOS Virtual Data center, 〈http://db.cosmos-eq.org/scripts/default.plx〉.
[39] National Geophysical Data Center (NGDC), 〈http://www.ngdc.noaa.gov〉.
[40] Earthquake Planning and Protection Organization. Greek Aseismic Code EAK2000. Greece: Athens; 2000.
[41] Eurocode 8: Design of structures for earthquake resistance. Part 1: General rules, seismic actions and rules for buildings. Brussels: European Committee for Standardization; 2004.
[42] Jennings PC. Ground motion parameters that influence structural damage. In: Scholl RE, King JL, editors. Strong ground motion simulation and engineering applications, EERI Publication 85-02. Berkeley, CA: Earthquake Engineering Research Institute; 1985.
[43] Fajfar P, Vidic T, Fischinger M. A measure of earthquake motion capacity to damage medium-period structures. Soil Dyn Earthquake Eng 1990;9(5):236–42.

[44] National Research Council. Review of recommendations for probabilistic seismic hazard analysis—quidance on uncertainty and use of experts. Panel on Seismic Hazard Analysis, Committee on Seismology, Board on Earth Sciences, Commission on Physical Sciences, Mathematics, and Resources, National Academy Press, Washington DC; 1997. p. 73.
[45] Benjamin JR and Associates. A criterion for determining exceedance of the operating basis earthquake, EPRI Report NP-5930, Electric Power Research Institute, Palo Alto, CA, 1988.
[46] Akkar S, Özen Ö. Effect of peak ground velocity on deformation demands for SDOF systems. Soil Dyn Earthquake Eng 2005;34: 1551–71.
[47] Travasarou T, Bray JD, Abrahamson NA. Empirical attenuation relationship for Arias Intensity. Earthquake Eng Struct Dyn 2003; 32(7):1133–55.
[48] Trifunac MD, Brady AG. A study on the duration of strong earthquake ground motion. Bull Seismol Soc Am 1975;65:581–626.
[49] Husid DE. Características de terremotos–Análisis general. Revista del IDIEM 1969;8:21–42.
[50] Ambraseys N, Smit P, Sigbjornsson R, Suhadolc P, Margaris B. Internet-Site for European Strong-Motion Data (IS-ESD). European Commission 2002, Research-Directorate General, Environment and Climate Programme, 〈http://www.isesd.cv.ic.ac.uk/ESD/frameset.htm〉.
[51] Gazetas G. Soil dynamics and earthquake engineering. Athens: Symeon editions; 1996 (in Greek).
[52] Krawinkler H, Alavi B. Development of improved design procedures for near-fault ground motions. In: SMIP98, seminar on utilization of strong motion data, Oakland, CA; 1998.
[53] Papazachos B, Papazachou C. The earthquakes of Greece. Thessaloniki: Ziti editions; 1997.
[54] Stewart JP, Chiou SJ, Bray JD, Graves RW, Somerville PG, Abrahamson NA. Ground motion evaluation procedures for performance-based design. PEER report 2001/09, 2001.
[55] Decanini L, Liberatore L, Mollaioli F. Estimation of near-source ground motion and seismic behaviour of RC framed structures damaged by the 1999 Athens earthquake. J Earthquake Eng 2005; 9(5):609–35.